Generalization of Rosenfeld's functional to non-additive hard-spheres: pair structure and test-particle consistency

2010 J. Phys.: Condens. Matter 22 035103

(http://iopscience.iop.org/0953-8984/22/3/035103)

IOP PUBLISHING JOURNAL OF PHYSICS: CONDENSED MATTER

J. Phys.: Condens. Matter **22** (2010) 035103 (8pp) doi:10.1088/0953-8984/22/3/035103

Generalization of Rosenfeld's functional to non-additive hard-spheres: pair structure and test-particle consistency

A Ayadim and S Amokrane

Physique des Liquides et Milieux Complexes, Faculté des Sciences et Technologie, Université Paris-Est (Créteil), 61 Avenue du Général de Gaulle, 94010 Créteil Cedex, France

Received 6 October 2009, in final form 13 November 2009
Published 21 December 2009
Online at stacks.iop.org/JPhysCM/22/035103

Abstract

The accuracy of the structural data obtained from the recently proposed generalization to non-additive hard-spheres (Schmidt 2004 *J. Phys.: Condens. Matter* **16** L351) of Rosenfeld's functional is investigated. The radial distribution functions computed from the direct correlation functions generated by the functional, through the Ornstein–Zernike equations, are compared with those obtained from the density profile equations in the test-particle limit, without and with test-particle consistency. The differences between these routes and the role of the optimization of the parameters of the reference system when the functional is used to obtain the reference bridge functional are discussed in the case of symmetric binary mixtures of non-additive hard-spheres. The case of highly asymmetric mixtures is finally briefly discussed.

1. Introduction

The application of the density functional theory (DFT) of classical systems requires the development of flexible functionals. This is especially important when DFT is used to obtain structural properties from the method of the test particle. Several successful functionals have been proposed in recent years for simple models such as the hard-sphere mixtures, the Lennard-Jones (LJ) or the Yukawa potential, but a generic functional capable of treating general interaction potentials beyond the mean field is still lacking (see for e.g. the review by Evans [2]; for more recent references see for example [3]). For this reason, methods based on the knowledge of the functional for some reference systems are very useful. This is the case with the approach pioneered by Rosenfeld [4], who proposed to use, for the unknown *bridge* functional, that of additive hard-spheres (HS) (the so-called fundamental measures functional (FMF)). Besides the HS mixture [5], this method has been used to study the LJ fluid [6], slightly asymmetric mixtures with various interactions [7], the potential of mean force (PMF) for colloids in the bulk [8] and in confined geometry [9, 10], up to the drying phenomenon [11] and spherically averaged anisotropic potentials [12]. Under the designation of reference functional approximation (RFA), we recently demonstrated [13] how it can be used to compute bulk free energies. The result improves upon the standard approximation of the non-local term in the reference hypernetted chain (RHNC) theory of Lado [14, 15]. Although being successful for a variety of interaction potentials, the original FMF may, however, be insufficient in some conditions. This is the case, for example, with the potential of mean force for certain highly asymmetric mixtures with attractive forces [8] (see also the discussion in [16] for hard-sphere mixtures). In the same theoretical framework, Schmidt has generalized the FMF to bonded potentials [17], soft ones [18], and more recently [1] to non-additive hard-spheres (NAHS). The first are discussed in [19] (the connection between the weight functions and the 'geometrical' properties of the particles is then not as simple as for hard-spheres—see for example [20]). In [1], it was shown that the NAHS functional gives an accurate description of the structure when the direct correlation functions (dcfs) computed as the second functional derivatives are inserted in the Ornstein–Zernike (OZ) equations [21]. Since he did not consider the test-particle limit, we do this here to further assess this method (we are not aware of tests other than Schmidt's calculations). Furthermore, since this procedure is limited to the NAHS mixture, one needs to invoke the RFA to study more general models with this functional. A conclusive test in this context would considerably extend its potential use. To this end, we first recall in section 2 the theoretical basis of this method. In section 3, we present a comparison of the different routes for the structure of the NAHS mixture. We also briefly

discuss the case of high size asymmetry. Section 4 summarizes our conclusions.

2. Theoretical background

2.1. General outline of the reference functional approach

The basis of the reference functional approximation is discussed in Rosenfeld's paper [4]. We briefly recall here the main steps of its implementation (see also [7, 13] for details). The starting point consists in devising some approximation for the excess free energy functional $F^{\rm ex}[\rho]$ for an inhomogeneous fluid whose particles are subject to an external potential $V_i(\mathbf{r})$ (in what follows, $F[\rho]$ designates a functional of the inhomogeneous density $\rho(\mathbf{r})$, which in a mixture corresponds to a set of densities $\{\rho_i(\mathbf{r})\}$). From the intrinsic free energy functional $F[\rho]$, the excess part $F^{\rm ex}[\rho]$ with respect to the ideal gas is defined as

$$F^{\rm ex}[\rho] \equiv F[\rho] - k_{\rm B}T \sum_i \int {\rm d}\mathbf{r}\, \rho_i(\mathbf{r})(\ln \rho_i(\mathbf{r})\Lambda_i^3 - 1), \quad (1)$$

where $k_{\rm B}$ is the Boltzmann constant, T is the absolute temperature and Λ_i is the thermal de Broglie wavelength. Useful approximations are obtained starting from the functional Taylor expansion of $F^{\rm ex}[\rho]$ about some reference density ρ_0. The coefficients of the expansion are the n-body direct correlation functions $c^{(n)}$ for species $k, \ldots, l$, defined by $c^{(n)}_{k,\ldots,l}(\mathbf{r}_1, \ldots, \mathbf{r}_n) = -\frac{\delta^{(n)}\beta F^{\rm ex}[\{\rho_i(\mathbf{r})\}]}{\delta\rho_k(\mathbf{r}_1)\cdots\delta\rho_l(\mathbf{r}_n)}$ (with $\beta = 1/k_{\rm B}T$), evaluated for $\rho_0(\mathbf{r})$. The contributions up to second order in the density difference $\Delta\rho_i(\mathbf{r}) = \rho_i(\mathbf{r}) - \rho_{i,0}(\mathbf{r})$ are collected in the contribution $F^{(2)}[\rho]$, usually referred to as the hypernetted chain (HNC) functional:

$$F^{(2)}[\rho] = F^{\rm ex}[\rho_0] - k_{\rm B}T \sum_i \int {\rm d}\mathbf{r}\, c_i^{(1)}(\mathbf{r}, \rho_0)\Delta\rho_i(\mathbf{r}) - \tfrac{1}{2}k_{\rm B}T \sum_{i,j} \int {\rm d}\mathbf{r}\, {\rm d}\mathbf{r}' c_{i,j}^{(2)}(\mathbf{r}, \mathbf{r}', \rho_0)\Delta\rho_i(\mathbf{r})\Delta\rho_j(\mathbf{r}') \quad (2)$$

and the terms beyond second order define the bridge functional [4]:

$$F^{\rm B}[\rho] \equiv F^{\rm ex}[\rho] - F^{(2)}[\rho]. \quad (3)$$

To go further, one needs some prescription for $F^{\rm B}$. In the reference functional approximation, it is replaced by the bridge functional of a reference system, $F^{\rm B,ref}$, for which $F^{\rm ex,ref}$ (and hence also $F^{(2),\rm ref}$) are known:

$$F^{\rm B,ref}[\rho] \equiv F^{\rm ex,ref}[\rho] - F^{(2),\rm ref}[\rho]. \quad (4)$$

In the fundamental measures theory [4] for additive hard-spheres, the excess functional is taken as

$$F^{\rm ex,HS}[\{\rho_i(\mathbf{r})\}] = k_{\rm B}T \int {\rm d}\mathbf{x}\, \Phi(\{n_\alpha(\mathbf{x})\}), \quad (5)$$

where $\{n_\alpha(\mathbf{x})\}$ is a set of weighted densities constructed from the actual densities $\rho_i(r)$ and weight functions $\omega_i^{(\alpha)}$ as $n_\alpha(\mathbf{x}) = \sum_i \rho_i \otimes \omega_i^{(\alpha)}$, where $\otimes$ designates the convolution product $[f \otimes g](\mathbf{r}) = \int {\rm d}\mathbf{r}'\, f(\mathbf{r}') * g(\mathbf{r} - \mathbf{r}')$.

In [1], Schmidt extended this method to non-additive hard-spheres, i.e. when the cross diameter is $\sigma_{ij} = \frac{1}{2}(\sigma_i + \sigma_j)(1+\delta)$. To this end, equation (5) is generalized as (for a binary mixture)

$$F^{\rm ex,NAHS}[\rho_1, \rho_2] = k_{\rm B}T \int {\rm d}\mathbf{x}_1 \int {\rm d}\mathbf{x}_2 \sum_{\alpha,\gamma=0}^{3} K_{\alpha\gamma}^{(12)}(|\mathbf{x}_1 - \mathbf{x}_2|) \times \Phi_{\alpha\gamma}(\{n_\nu^{(1)}(\mathbf{x}_1)\}, \{n_\tau^{(2)}(\mathbf{x}_2)\}), \quad (6)$$

where the functions $\Phi_{\alpha\gamma}$ depend on weighted densities $n_\alpha^{(i)}(\mathbf{x}) = \rho_i \otimes \omega_i^{(\alpha)}$, one for each type of particle. The weight functions are the purely scalar Kierlik–Rosinberg ones [22]. The kernels $K_{\alpha\gamma}^{(12)}$ correlate the weighted densities for component (1) at $\mathbf{x}_1$ with those of component (2) at $\mathbf{x}_2$ (note the strict correspondence between the coordinates $\mathbf{x}_1$, $\mathbf{x}_2$ and the species numbers). They involve the delta function and its derivatives, up to the fifth order. Although the calculations involve no special difficulty, the algebra is rather tedious given the number of $\binom{\nu\tau}{\alpha\gamma}$ derivatives one needs to consider—each $\Phi_{\alpha\gamma}$ involving 28 terms (detailed expressions are given in [1]).

From $F^{\rm ex,ref}[\rho]$ (where ref $\equiv$ HS or NAHS), one evaluates the coefficients $c_i^{(1),\rm ref}$ and $c_{ij}^{(2),\rm ref}$ of the functional $F^{(2),\rm ref}$ (one- and two-particle dcfs) and thus determine $F^{\rm B,ref}$. The excess free energy in the RFA is thus

$$F^{\rm ex}[\rho] \simeq F^{(2)}[\rho] + F^{\rm B,ref}[\rho]. \quad (7)$$

2.2. Computing the structure from the functional

2.2.1. Pair structure from the direct correlation functions. From the functional $F^{\rm ex}$ in equation (7) one can compute the 2-body dcfs in the bulk as

$$c_{ij}^{(2),\rm FD}(|\mathbf{r}_1 - \mathbf{r}_2|) = -\frac{\delta^{(2)}\beta F^{\rm ex}[\{\rho_i(\mathbf{r})\}]}{\delta\rho_i(\mathbf{r}_1)\delta\rho_j(\mathbf{r}_2)}\bigg|_{\rho_i^0,\rho_j^0}, \quad (8)$$

where ρ_i^0 and ρ_j^0 are the bulk densities. The label FD is used to distinguish them from the ones defined by the Ornstein–Zernike equations:

$$h_{ij} = c_{ij} + \sum_k \rho_k c_{ik} \otimes h_{kj} \quad (9)$$

together with the closure relations

$$g_{ij} = \exp\{-\beta\phi_{ij} + h_{ij} - c_{ij} - b_{ij}\}, \quad (10)$$

with $g_{ij} = h_{ij} + 1$ the radial distribution functions (rdf)—assuming interaction potentials ϕ_{ij} with spherical symmetry and b_{ij} the bridge functions. As a first step, one may estimate the correlation functions as $h_{ij}^{\rm FD} = c_{ij}^{(2),\rm FD} + \sum_k \rho_k c_{ik}^{(2),\rm FD} \otimes h_{kj}^{\rm FD}$, without using the closures. The convolutions are readily performed in Fourier space, and from the inverse transforms one gets $g_{ij}^{\rm FD} = h_{ij}^{\rm FD} + 1$. This is the method used by Schmidt to test his functional at the level of the structure.

2.2.2. Pair structure from the density profile equations. Within DFT, the second route for computing the bulk structure uses the test-particle method due to Percus [23]. One starts with the equation for the density profile $\rho_i(\mathbf{r})$ for species i

subject to an external potential $V_i(\mathbf{r})$. By minimizing the grand potential $\Omega[\rho] = F[\rho] - \sum_i \int d\mathbf{r}\, \rho_i(\mathbf{r})(\mu_i - V_i(\mathbf{r}))$, one gets

$$\rho_i(\mathbf{r}) = \rho_i^0 \exp\{-\beta V_i(\mathbf{r}) + c_i^{(1)}(\mathbf{r}) - c_{i,o}^{(1)}(\mathbf{r})\}, \tag{11}$$

where ρ_i^0 is the density of particles of type i far from the inhomogeneity and $c_i^{(1)}(\mathbf{r}_1) = -\frac{\delta\beta F^{\rm ex}[\{\rho_i(\mathbf{r})\}]}{\delta\rho_i(\mathbf{r}_1)}$ is the one particle direct correlation function ($\mu_{i,\rm ex}[\{\rho_i(\mathbf{r});\mathbf{r}\}] = -k_{\rm B}Tc_i^{(1)}$ is the excess chemical potential functional). When the inhomogeneity is created by a test particle t at $\mathbf{r}_0$ (say the origin), such that $V_i(\mathbf{r}) = \phi_{it}(\mathbf{r}-\mathbf{r}_0)$, with ϕ_{it} the pair potential acting between particles of species i and t, the density profile is $\rho_i(\mathbf{r}) = \rho_i^0 g_{it}(\mathbf{r})$, where $g_{it}(\mathbf{r})$ is the distribution function for the pair (i,t). This second estimation of the rdf:

$$g_{it}^{\rm DP} = \exp\{-\beta(\phi_{ij} + (\mu_{i,\rm ex}[\{\rho_j(\mathbf{r})\};\mathbf{r}] - \mu_{i,\rm ex}(\{\rho_j^0\}))\} \tag{12}$$

is labeled by DP to emphasize that it follows from the density profile equation. At this stage, the OZ equation is not used. The latter is formally introduced by using in the density profile equation the expansion (1)–(3) to get

$$g_{it}(\mathbf{r},\mathbf{r}_0) = \exp\{-\beta\phi_{it}(\mathbf{r},\mathbf{r}_0) + h_{it}(\mathbf{r},\mathbf{r}_0) - c_{it}(\mathbf{r},\mathbf{r}_0) - b_{it}(\mathbf{r},\mathbf{r}_0)\} \tag{13}$$

in which the bridge functions $b_{it}(\mathbf{r},\mathbf{r}_0) = \beta\frac{\delta F^{\rm B}}{\delta\rho_i(\mathbf{r})}|_{\rho_i=\rho_0 g_{ij}}$ are obtained as the functional derivatives of the bridge functional $F^{\rm B}$, equation (3). In the RFA, replacing $F^{\rm B}$ by $F^{\rm B,ref}$ (with ref ≡ HS or NAHS for example) replaces the unknown exact bridge function by the one computed from the reference functional $b_{it}^{\rm ref}$. This is emphasized in the corresponding rdf (for spherically symmetric potentials and a test particle placed at the origin):

$$g_{ij}^{\rm RFA}(r) = \exp\{-\beta\phi_{ij} + h_{ij} - c_{ij} - b_{ij}^{\rm ref}\}. \tag{14}$$

This expression is similar [4] to the RHNC closure [14] of the OZ equations (for a detailed discussion of the differences see [13]). When the bridge function is, as $b_{ij}^{\rm ref}$, obtained from a free energy functional, this route to the structure is often referred to as the test-particle consistent DFT.

In the RFA, one needs to specify the parameters of the reference system (here the hard-sphere diameters σ_{ij}). We consider here the Lado criterion [24] generalized to mixtures [7]. For non-additive hard-spheres, one also has to minimize with respect to the cross diameter (i.e. the non-additivity parameter δ). By defining $\sigma_{33} \equiv \delta$ the three coupled equations read

$$\sum_{ij}\rho_i\rho_j\int d\mathbf{r}\,[g_{ij}(r) - g_{ij}^{\rm ref}(r)]\frac{\partial b_{ij}^{\rm ref}[\{g_{ij}\};r]}{\partial\sigma_{kk}} = 0; \quad k = 1,3. \tag{15}$$

This simplified criterion is more convenient than the one strictly consistent with the RFA, as discussed in [13]. As an alternative, we will also consider the virial-compressibility consistency:

$$\left(\frac{\partial\beta P}{\partial\rho}\right)_T = 1 - \rho\sum_{i,j}x_i x_j\widetilde{c}_{ij}(k=0), \tag{16}$$

where P is the virial pressure, $\widetilde{c}_{ij}(k)$ is the Fourier transform of the dcf and x_i is the mole fraction of component i. This criterion allows the determination of one parameter (more if partial compressibilities are used).

The degree of agreement between $g_{ij}^{\rm FD}$, $g_{ij}^{\rm DP}$ and $g_{ij}^{\rm RFA}$ measures the internal consistency of an approximate functional. Their respective accuracy can be checked by comparison with exact results. Another aspect is the amount of numerical work they require. Since the OZ equations must be solved for each set of reference system parameters, the latter being determined from the above criteria, computing $g_{ij}^{\rm RFA}$ is by far more complex than $g_{ij}^{\rm FD}$ and $g_{ij}^{\rm DP}$ (the easiest one being $g_{ij}^{\rm FD}$ since it does not require iterations). We present in the next sections some calculations illustrating these points.

3. Results and discussion

3.1. DCF from the functional derivative versus the test-particle route

The comparison $g_{ij}^{\rm FD}$ versus $g_{ij}^{\rm DP}$ will illustrate one important consequence of using $F^{\rm ex,NAHS}[\rho]$ in the test-particle limit. The variables are here the packing fractions $\eta_i = \frac{\pi}{6}\rho_i\sigma_{ii}^3$. The total reduced density is $\rho^* = \rho_1\sigma_{11}^3 + \rho_2\sigma_{22}^3$. Figure 1(a) shows these functions for one state point considered by Schmidt: at this scale, they are nearly indistinguishable. On an enlarged one, however, $g_{ij}^{\rm DP}(r)$ shows irregularities (discontinuities in the function or its slope) that do not exist in $g_{ij}^{\rm FD}$. By considering different mesh sizes in direct and reciprocal space and number of grid points (up 32 768) we have checked that these are not numerical artifacts. Their origin is related to the derivatives of the Dirac delta function involved in $K_{\alpha\gamma}^{(12)}$ when they are convoluted with functions which present discontinuities or have a discontinuous slope. An example is the following contribution

$$\mu_2^*(\mathbf{r}) = \int d\mathbf{x}\, w_2^{(2)}(|\mathbf{x}-\mathbf{r}|)\int d\mathbf{x}'\sum_{\alpha,\gamma}K_{\alpha\gamma}^{(12)}(|\mathbf{x}-\mathbf{x}'|) \times\left[\frac{\partial\Phi_{\alpha\gamma}}{\partial n_2^{(2)}} - \frac{\partial\Phi_{\alpha\gamma}}{\partial n_{2,0}^{(2)}}\right](\mathbf{x},\mathbf{x}') \tag{17}$$

to the chemical potential functional of species 2 (see the appendix). The result $H(x)$ of the integration with respect to $\mathbf{x}'$ is shown in figure 1(b). Due to the use of discretized Fourier transforms, delta singularities show up as finite height spikes. The integrations are insufficient to smooth the effect of the $\delta^{(n)}$ derivatives in $K_{\alpha\gamma}$ convoluted with the discontinuous functions $\Phi_{\alpha\gamma}$, even after the final convolution with $w_2^{(2)}$ (figure 1(c)). Despite some global constraints obeyed by the functional, the resulting discontinuities cannot be canceled by other contributions to the chemical potential functional, since they have completely different structures (a formal proof would however be non-trivial). This problem with weights involving delta functions—here also in $K_{\alpha\gamma}$—is not unusual and similar observations were made in [25, 26]. Such irregularities are absent in the additive case (FMF with Kierlik–Rosinberg weights) since possible discontinuities in the integrands of the chemical functionals occur either

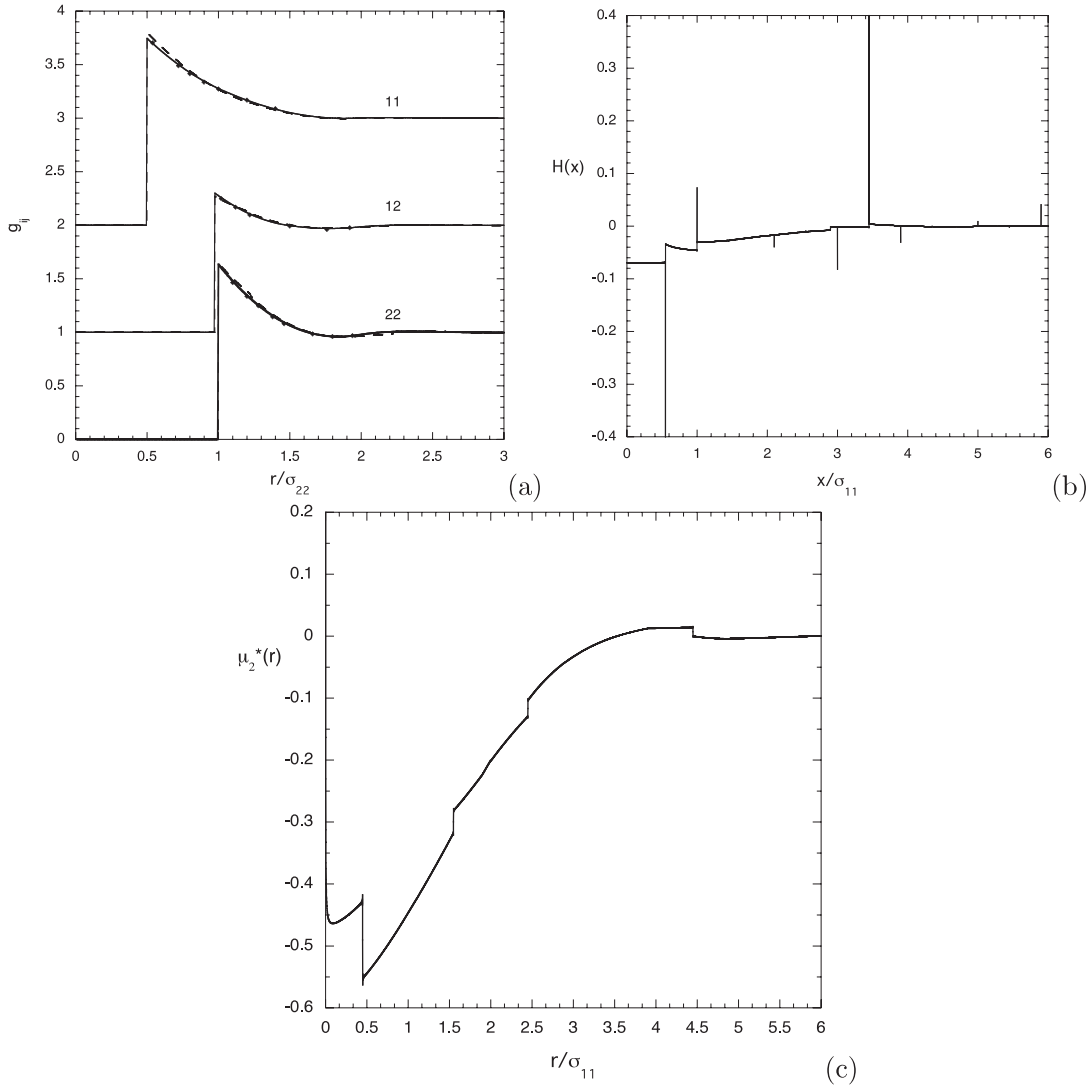

Figure 1. (a) Radial distribution functions of a mixture of non-additive hard-spheres from the direct correlation function (FD) and the test-particle method (DP). The same parameters as figure 2 in [1] (note our convention '2' ≡ big): size ratio $\sigma_{22}/\sigma_{11} = 2$, $\delta = 0.3$, $\eta_2 = 0.05$, $\eta_1 = \eta_2/8$. The data for g_{12} and g_{11} are shifted by 1 and 2 units, respectively. Solid line: FD; dashed line: DP; symbols: simulations. (b) Integrand of equation (17) (first integration with respect to $\mathbf{x}'$). (c) Final contribution of equation (17) to the chemical potential functional for species 2. Jumps occur at some multiples of the radius $\sigma_{11}/2$ and some combinations involving also $\sigma_{22}/2$ and δ.

in the region where the weighted densities are uniform or beyond the location of the $\delta^{(n)}$ singularities). In contrast with what occurs in this test-particle route, only *uniform* densities are involved when computing g_{ij}^{FD} from $c_{ij}^{(2),\mathrm{FD}}$. The functions $\Phi_{\alpha\gamma}(\{n_\nu^{(1)}(\mathbf{x}_1)\}, \{n_\tau^{(2)}(\mathbf{x}_2)\})$ are then uniform, and the integration of $K_{\alpha\gamma}^{(12)}(|\mathbf{x}_1 - \mathbf{x}_2|)$ gives a constant. Accordingly, $c_{ij}^{(2),\mathrm{FD}}(r)$ shows a smooth variation with separation, besides the discontinuity at the hard core, as in the additive case. As illustrated here (in the conditions of figure 1(a)), this effect is not important. This may no longer be the case at higher asymmetry or greater non-additivity. We do not see at present how to correct this with simple modifications of the coefficients $K_{\alpha\gamma}^{(12)}$.

3.2. Test-particle consistency

We now consider the rdf g_{ij}^{RFA}, which makes use of the bridge functional for non-additive hard-spheres. In this case, we also need to determine the reference system parameters. We first discuss, as a special case, additive hard-spheres.

3.2.1. Additive hard-spheres. To test the optimization by equations (15) and (16), we considered a binary mixture of *additive* hard-spheres, treated with the bridge functional for *non-additive* hard-spheres. In the additive mixture, the diameters are σ_{11}, σ_{22} and $\sigma_{12} = \frac{1}{2}(\sigma_{11} + \sigma_{22})$. We denote by $\widetilde{\sigma}_{11}$, $\widetilde{\sigma}_{22}$ and $\widetilde{\sigma}_{12} = \frac{1}{2}(\widetilde{\sigma}_{11} + \widetilde{\sigma}_{22})(1 + \widetilde{\delta})$ the corresponding (variational) ones in the reference system. For a non-additivity parameter $\delta = 0$, and before test-particle consistency, Schmidt's functional reduces to the additive HS one. However, it is not *a priori* certain that the optimum parameters would be the actual ones (i.e. $\widetilde{\sigma}_{11} = \sigma_{11}$; $\widetilde{\sigma}_{22} = \sigma_{22}$; $\widetilde{\delta} = \delta = 0$) after imposing the consistency. Indeed, in order to be true, this requires that $\frac{\partial b(r)}{\partial \widetilde{\delta}}|_{\widetilde{\delta}=0}$ should also vanish while the derivatives with respect to $\widetilde{\sigma}_{11}$ and $\widetilde{\sigma}_{22}$ should go into those for

Table 1. Radial distribution function of a symmetric mixture of non-additive hard-spheres. $\rho\sigma^3$ is the total reduced density, δ the actual non-additivity parameter and $\widetilde{\delta}$ the optimized one in the RFA, subscripts $(2a)$ and $(2b)$ corresponding to the Lado criterion and the virial-compressibility consistency respectively. Subscript (1) is for the original FMF (additive case). The simulation data (MC) and the results of the Ballone–Pastore–Galli–Gazzillo (BPGG) integral equation [30] are from [27].

		$\delta = 0.05$			$\delta = 0.1$		
$\rho\sigma^3$	Source	$g_{11}(d_{11})$	$g_{12}(d_{12})$	$\widetilde{\delta}$	$g_{11}(d_{11})$	$g_{12}(d_{12})$	$\widetilde{\delta}$
0.2	MC	1.390	1.310		1.420	1.360	
	BPGG	1.373	1.328		1.436	1.331	
	$\text{RFA}_{(1)}$	1.377	1.329		1.443	1.330	
	FD	1.364	1.321		1.425	1.326	
	DP	1.374	1.327		1.436	1.325	
	$\text{RFA}_{(2a)}$	1.367	1.321	0.092	1.426	1.316	0.130
	$\text{RFA}_{(2b)}$	1.377	1.329	−0.012	1.444	1.331	−0.01
0.4	MC	2.050	1.820		2.24	1.79	
	BPGG	1.993	1.822		2.211	1.793	
	$\text{RFA}_{(1)}$	2.005	1.819		2.255	1.771	
	FD	1.932	1.787		2.149	1.774	
	DP	2.003	1.816		2.253	1.747	
	$\text{RFA}_{(2a)}$	1.967	1.791	0.057	2.160	1.723	0.092
	$\text{RFA}_{(2b)}$	2.015	1.825	−0.014	2.284	1.780	−0.031
0.6	MC	3.150	2.560		3.900	2.230	
	BPGG	3.119	2.579		3.712	2.344	
	$\text{RFA}_{(1)}$	3.160	2.546		3.911	2.187	
	FD	2.898	2.479		3.419	2.498	
	DP	3.217	2.526				
	$\text{RFA}_{(2a)}$	3.018	2.461	0.040	3.350	2.010	0.071
	$\text{RFA}_{(2b)}$	3.197	2.565	−0.012	4.104	2.214	−0.048

additive HS. We have checked that this is not actually the case, except at low density (to simplify the calculation, we used g_{ij}^{FD} for $g_{ij}^{\text{ref}}(r)$ in equation (15)). The limiting behavior for $\delta \to 0$ of the generalized functional is thus not preserved in the test-particle consistent calculation, with optimization according to Lado's criterion. This particular behavior, in particular that of $\frac{\partial b(r)}{\partial \delta}|_{\widetilde{\delta}=0}$, led us to consider determining $\widetilde{\delta}$ from the alternative criterion (16). We examine this below, starting with symmetric mixtures.

3.2.2. Symmetric mixture of non-additive hard-spheres. The case $\sigma_{11} = \sigma_{22}$ and $\delta \neq 0$ has been considered numerous times in the literature (see references in [1, 7, 27, 28] for DFT or integral equations and [29] for recent simulations). We reconsider it here to study the role of the test-particle consistency in the non-additive HS functional. In table 1, we show the contact values computed for some of the state points considered by Gazzillo [27]. The role of the test-particle consistency can be analyzed by comparing the lines labeled DP and RFA (with subscripts (1) and (2) for the additive and non-additive cases respectively).

Quite generally, the functional for non-additive hard-spheres works rather well over the parameter ranges in table 1, when the optimum non-additivity parameter is obtained from the virial-compressibility consistency ($\text{RFA}_{(2b)}$). Note that some state points are very close to or even inside the spinodal computed from the compressibility route (vanishing of $(1 - \rho_1\widetilde{c}_{11})(1 - \rho_2\widetilde{c}_{22}) - \rho_1\rho_2\widetilde{c}_{12}^2$) at $k = 0$). One example is the case $\rho^* = 0.6$ and $\delta = 0.1$. Poles at $k \neq 0$ then start to develop in the Fourier transforms $\widetilde{c}_{ij}(k)$ used to compute the bridge functions (see the appendix). As discussed in [31], similar poles are not seen numerically due to the finite mesh size. The fact that g^{RFA} remains acceptable even in such pathological cases testifies of the robustness of the integral equations route (here test-particle consistent DFT)—in contrast to the FD or DP ones. This is particularly evident in figure 2, which shows

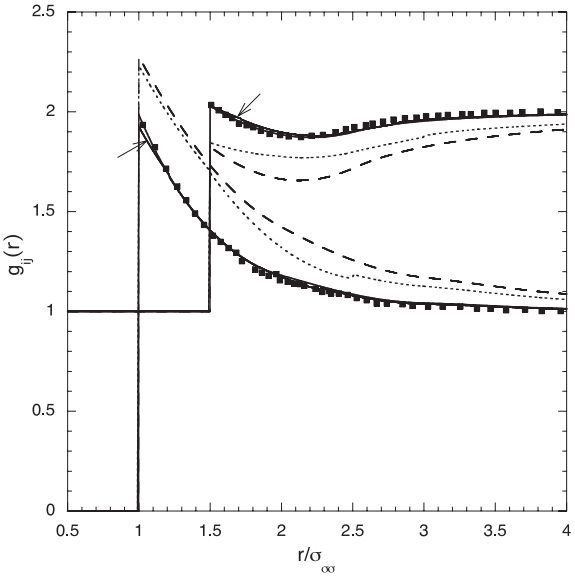

Figure 2. Comparison of the three routes to the radial distribution functions of a symmetric mixture of non-additive hard-spheres. The curves for g_{12} are shifted by one unit. Solid curves: RFA_{1-2} (those with Schmidt's functional are indicated by an arrow). Dotted curves: DP, dashed curves: FD. Symbols: simulations. The parameters are $\rho^* = 0.15$, $x_2 = 0.5$, $\delta = 0.5$ (as in figure 3(d) of [7]).

the rdf for one of the state points considered by Kahl *et al* [7]. They have shown that the additive HS functional is accurate in the situations they investigated. Figure 2 shows that, in the same conditions, the non-additive one does equally well—in the test-particle consistent route. The poor results obtained in its absence (g_{ij}^{FD} and g_{ij}^{DP}) highlight the crucial importance of the consistency imposed by the Ornstein–Zernike equations.

3.2.3. Highly asymmetric mixtures. We finally briefly consider the case $\sigma_{22} \gg \sigma_{11}$. In figure 3 we show g_{ij}^{FD} and g_{ij}^{DP} for $\sigma_{22}/\sigma_{11} = 10$ and a state point very close to the compressibility spinodal. We checked that our values of the structure factors $S_{ij}(k)$ are the same as in figure 4 in [1]. For this size asymmetry, the value of $S_{ij}(k)$ near the spinodal is extremely sensitive to the numerical details (see our previous discussion [32] for additive hard-spheres). Although criteria such as exact sum rules should be better indicators, we consider this as a confirmation of the correct implementation of the functional already evidenced by the results in figure 1 for $\sigma_{22}/\sigma_{11} = 2$. Again we observe an important difference between g_{ij}^{FD} and g_{ij}^{DP}. We cannot compute g_{ij}^{RFA} for this point which is in the non-convergence domain of the RFA integral equation. Note that taking $\delta = 0.5$ for $\sigma_{22}/\sigma_{11} = 10$ corresponds to a strong non-additivity at the scale of the small spheres ($2.25\sigma_{11}$), which is a severe condition for the functional. To illustrate the effect of the consistency we consider a less asymmetric situation in which the RFA converges. An example is shown in figure 4 for $\sigma_{22}/\sigma_{11} = 5$, $\delta = 0.2$, $\eta_1 = 0.01$ and $\eta_2 = 0.15$. In order to illustrate the role of the different parameters, three different steps of a typical RFA calculation are illustrated, the reference being g_{ij}^{DP}. The original functional (RFA_1) is first used. The Lado criterion is approximately satisfied for $\widetilde{\sigma}_{11} = 1.2\sigma_{11}$, $\widetilde{\sigma}_{22} = 0.91\sigma_{22}$. Good agreement with g_{ij}^{DP} is then found. Turning to the functional for the non-additive hard-spheres (RFA_2), we first keep the same values of $\widetilde{\sigma}_{11}$ and $\widetilde{\sigma}_{22}$ and use $\widetilde{\delta} = \delta$. The result then differs greatly from g_{ij}^{DP}. For this value of $\widetilde{\delta}$, a better agreement is on the contrary found for $\widetilde{\sigma}_{11} = \sigma_{11}$ and $\widetilde{\sigma}_{22} = \sigma_{11}$. This confirms the necessity to optimize all the parameters of the reference functional. The best result is expected with (RFA_2), but we did not perform the full optimization because of the considerable amount of computer time that this requires (but which might, however, be necessary in specific situations).

To close this discussion we mention the combination of high asymmetry and attractive forces, that originally motivated this study. Indeed, [8], pointed out some difficulties with the FMF when computing the potential of mean force for macroparticles at infinite dilution for the model considered by Shinto *et al* [33]. Although one gains additional flexibility with the generalized functional, with a clear improvement upon the results of [8], we could not find a set of optimized parameters that permit a good description of the simulation data over the whole separation range. Besides the remarks raised above, we suspect that an additional difficulty then comes from the use of an optimization criterion for *homogeneous* mixtures. This point being not specific to the generalized functional, we defer its investigation to future work.

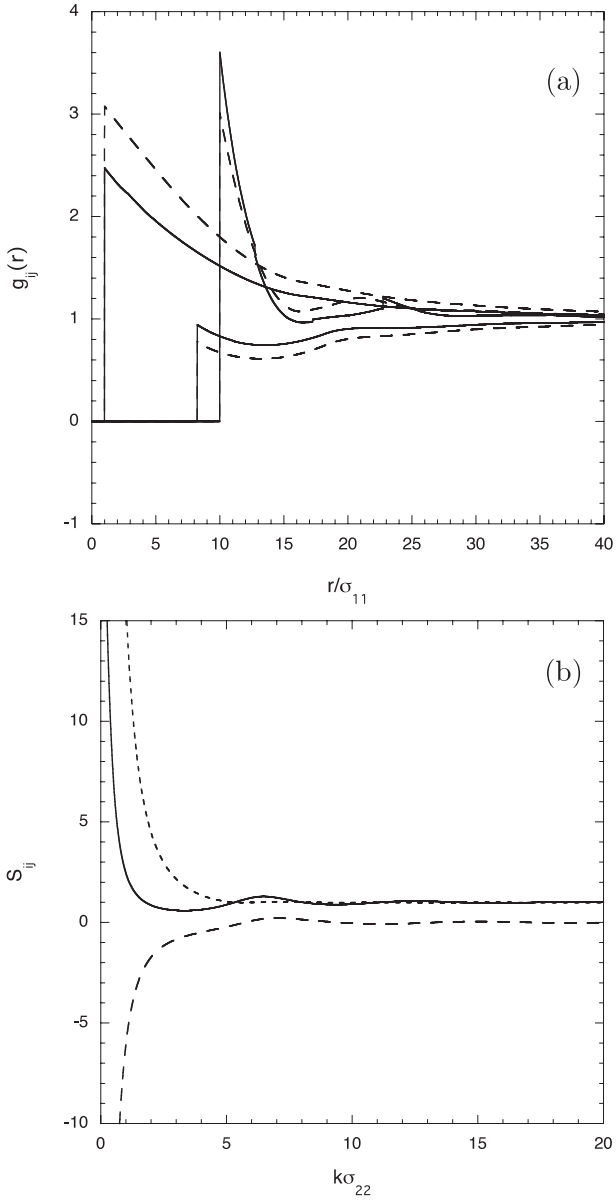

Figure 3. (a) Radial distribution functions of an asymmetric mixture of non-additive hard-spheres for $\sigma_{22}/\sigma_{11} = 10$. The parameters are $\rho^* = 0.164$, $x_2 = 0.189$, $\delta = 0.5$. Solid curves: DP, dashed curves: FD. (b) Structure factors of an asymmetric mixture of non-additive hard-spheres from the FD dcfs (equation (8)) for $\sigma_{22}/\sigma_{11} = 10$. The parameters are the same as in figure 3. Solid curve: $S_{22}(k)$; dotted curve: $S_{11}(k)$; dashed curve: $S_{12}(k)$.

4. Conclusion

In this work, we have examined the generalization to non-additive hard-spheres of the free energy functional based on the fundamental measures of the particles originally proposed by Rosenfeld.

Our results suggest that the form of the matrix **K** that controls the non–local character of the free energy density should be improved at least to eliminate some unwanted irregularities in the structural quantities derived in the test-particle route. In its present form, one must impose the test-particle consistency to obtain good results for the structure,

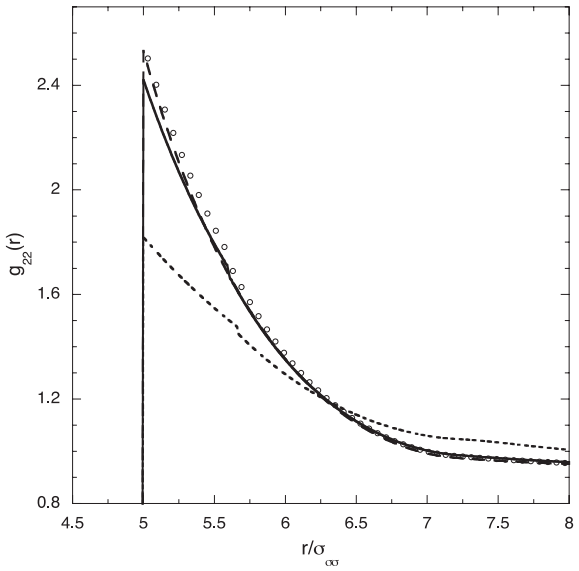

Figure 4. Radial distribution functions of an asymmetric mixture of non-additive hard-spheres. Solid curve: RFA$_{(2)}$ with $\widetilde{\sigma}_{11} = \sigma_{11}$, $\widetilde{\sigma}_{22} = \sigma_{22}$ and $\widetilde{\delta} = \delta$; dotted curve: RFA$_{(2)}$ with $\widetilde{\sigma}_{11} = 1.2\sigma_{11}$, $\widetilde{\sigma}_{22} = 1.09\sigma_{22}/1.2$ and $\widetilde{\delta} = \delta$; dashed curve: RFA$_{(1)}$; symbols: g_{22}^{DP}. The parameters are $\sigma_{22}/\sigma_{11} = 5$, $\delta = 0.2$, $\eta_2 = 0.15$ and $\eta_1 = 0.01$.

especially close to the spinodal. The non-additivity parameter should then be determined from the virial-compressibility consistency rather than from the Lado criterion. The results are then comparable to those of Rosenfeld's functional—slightly better for the correlation between unlike particles—but at the price of increased complexity. Together with some correction for the kernel matrix, other optimization criteria might be necessary to make this functional appropriate for non-standard interaction potentials, such as those encountered in the one-component description of soft matter fluids.

Appendix. Bridge function in the test-particle limit of the RFA

We give here the main steps in the computation of the bridge functions. From the definition $b_{it}(r) = \beta \frac{\delta F^{\mathrm{B}}}{\delta \rho_i(\mathbf{r})}|_{\rho_i = \rho_0 g_{ij}}$ one obtains in the RFA:

$$b_{ij}(r) = \beta(\mu_i^{\mathrm{ex,ref}}[\{\rho_i g_{ij}(\mathbf{r}); \mathbf{r}\}] - \mu_i^{\mathrm{ex,ref}}(\{\rho_i\})) + \sum_k \rho_k c_{ik}^{(2),\mathrm{ref}} \otimes h_{kj}(r) \tag{A.1}$$

with

$$\beta\mu_i^{\mathrm{ex,HS}}[\{\rho_i(r)\}; \mathbf{r}] = -c_i^{(1),\mathrm{HS}}(r) = \int \mathrm{d}\mathbf{r}' \sum_\alpha \frac{\partial \Phi}{\partial n_\alpha}[\{n_\alpha(r')\}; r]\omega_i^{(\alpha)}(\mathbf{r}' - \mathbf{r})$$

and

$$-c_{ij}^{(2),\mathrm{HS}}(\mathbf{r}) = \sum_{\gamma,\theta}\left[\frac{\partial^2 \Phi}{\partial n_\theta \partial n_\gamma}\right]_{\{n_\tau^0\}} \int \mathrm{d}\mathbf{r}'\, \omega_i^{(\theta)}(\mathbf{r}')\omega_j^{(\gamma)}(\mathbf{r}' - \mathbf{r})$$

$$-\widetilde{c}_{ij}^{(2),\mathrm{HS}}(k) = \sum_{\gamma,\theta}\left[\frac{\partial^2 \Phi}{\partial n_\theta \partial n_\gamma}\right]_{\{n_\tau^0\}} \widetilde{\omega}_i^{(\theta)}(\mathbf{k})\widetilde{\omega}_j^{(\gamma)}(-\mathbf{k}). \tag{A.2}$$

For non-additive hard-spheres one has instead

$$\frac{\delta F^{\mathrm{ex,NAHS}}}{\delta \rho_i(\mathbf{r})} = \sum_\gamma \int \mathrm{d}\mathbf{x}\, w_\gamma^{(i)}(|\mathbf{x} - \mathbf{r}|) \times \left[\int \mathrm{d}\mathbf{x}' \sum_{\alpha,\beta}^{3} K_{\alpha\beta}^{(12)}(|\mathbf{x} - \mathbf{x}'|)\frac{\partial \Phi_{\alpha\beta}}{\partial n_\gamma^{(i)}}(\mathbf{x}, \mathbf{x}')\right] \tag{A.3}$$

$$\frac{\delta^2 F^{\mathrm{ex,NAHS}}}{\delta \rho_i(\mathbf{r})\delta \rho_j(\mathbf{r}')} = \sum_{\gamma,\theta}^{3}\sum_{\alpha,\beta}^{3} \int \mathrm{d}\mathbf{x}\, w_\gamma^{(i)}(|\mathbf{x} - \mathbf{r}|) \times \left[\int \mathrm{d}\mathbf{x}' K_{\alpha\beta}^{(12)}(|\mathbf{x} - \mathbf{x}'|)\frac{\partial^2 \Phi_{\alpha\beta}}{\partial n_\gamma^{(i)} \partial n_\theta^{(j)}}(\mathbf{x}, \mathbf{x}') \times w_\theta^{(j)}(|\mathbf{x}' - \mathbf{r}'|)\right]. \tag{A.4}$$

Note that the densities $n^{(i)}$ must be evaluated at the same position $\mathbf{x}$, for $i = j$. All these convolutions are treated by Fourier transforms giving

$$-\widetilde{c}_{ij}^{(2),\mathrm{NAHS}}(k) = \sum_{\gamma,\theta}\sum_{\alpha,\beta} \frac{\partial^2 \Phi_{\alpha\beta}}{\partial n_\gamma^{(i)} \partial n_\theta^{(j)}}\bigg|_{\{n_\tau^{(j)0}\}} \times \widetilde{K}_{\alpha\beta}^{(12)}((1 - \delta_{ij})k)\widetilde{\omega}_i^{(\gamma)}(\mathbf{k})\widetilde{\omega}_j^{(\theta)}(-\mathbf{k}). \tag{A.5}$$

References

[1] Schmidt M 2004 *J. Phys.: Condens. Matter* **16** L351
[2] Evans R 1992 *Fundamentals of Inhomogeneous Fluids* ed D Henderson (New York: Dekker) chapter 3, p 85
[3] Löwen H 2002 *J. Phys.: Condens. Matter* **14** 11897
Kahl G and Löwen H 2009 *J. Phys.: Condens. Matter* **21** 464101
[4] Rosenfeld Y 1993 *J. Chem. Phys.* **98** 8126
[5] Rosenfeld Y 1994 *Phys. Rev. Lett.* **72** 3831
[6] Rosenfeld Y 1998 *Mol. Phys.* **94** 929
[7] Kahl G, Bildstein B and Rosenfeld Y 1996 *Phys. Rev.* E **54** 5391
[8] Amokrane S and Malherbe J G 2001 *J. Phys.: Condens. Matter* **13** 7199
Amokrane S and Malherbe J G 2002 *J. Phys.: Condens. Matter* **14** 3845 (erratum)
[9] Ayadim A, Malherbe J G and Amokrane S 2005 *J. Chem. Phys.* **122** 234908
[10] Amokrane S, Ayadim A and Malherbe J G 2007 *J. Phys. Chem.* C **111** 15982
[11] Oettel M 2005 *J. Phys.: Condens. Matter* **17** 429
[12] Mognetti B, Oettel M, Yelash L, Virnau P, Paul W and Binder K 2008 *Phys. Rev.* E **77** 041506
[13] Ayadim A, Oettel M and Amokrane S 2009 *J. Phys.: Condens. Matter* **21** 115103
[14] Lado F 1973 *Phys. Rev.* A **8** 2548
[15] Lado F, Foiles S M and Ashcroft N W 1983 *Phys. Rev.* A **28** 2374
[16] Botan V, Pesth F, Schilling T and Oettel M 2009 *Phys. Rev.* E **79** 061402
[17] Schmidt M 1999 *J. Phys.: Condens. Matter* **11** 10163
[18] Schmidt M 2000 *Phys. Rev.* E **62** 4976
[19] Rosenfeld Y, Schmidt M, Watzlawek M and Löwen H 2000 *Phys. Rev.* E **62** 5006
[20] Sweatman M B 2002 *J. Phys.: Condens. Matter* **14** 11921
[21] Hansen J P and McDonald I R 1976 *Theory of Simple Liquids* (London: Academic)
[22] Kierlik E and Rosinberg M L 1990 *Phys. Rev.* A **42** 3382
[23] Percus J K 1962 *Phys. Rev. Lett.* **11** 462
[24] Lado F 1982 *Phys. Lett.* **89** 196

[25] Gonzales A, White J A and Evans R 1997 *J. Phys.: Condens. Matter* **9** 2375
[26] Rosenfeld Y, Schmidt M, Löwen H and Tarazona P 1997 *Phys. Rev.* E **55** 4245
[27] Gazzillo D 1991 *J. Chem. Phys.* **95** 4565
Gazzillo D 1995 *Mol. Phys.* **84** 303
[28] Jagannathan K, Reddy G and Yethiraj A 2005 *J. Phys. Chem.* B **109** 6764
[29] Paricaud P 2008 *Phys. Rev.* E **78** 021202
[30] Ballone P, Pastore S, Galli G and Gazzillo D 1986 *Mol. Phys.* **59** 275
[31] Belloni L 1993 *J. Chem. Phys.* **98** 8080
[32] Ayadim A and Amokrane S 2006 *Phys. Rev.* E **74** 021106
[33] Shinto H, Miyahara M and Higashitani K 1999 *J. Colloid Interface Sci.* **209** 79–85